Published in final edited form as:
Brain Res Dev Brain Res. 2005 June 9; 157(1): 8–18. doi:10.1016/j.devbrainres.2005.02.017.

Neurogenesis and ontogeny of specific cell phenotypes within the hamster suprachiasmatic nucleus

Michael C. Antle[a,*], **Joseph LeSauter**[b], and **Rae Silver**[a,b,c]

[a]Department of Psychology, Columbia University, NY 10027, USA

[b]Department of Psychology, Barnard College, NY 10027, USA

[c]Department of Anatomy and Cell Biology, College of Physicians and Surgeons, Columbia University, NY 10032, USA

Abstract

The hamster suprachiasmatic nucleus (SCN) is anatomically and functionally heterogeneous. A group of cells in the SCN shell, delineated by vasopressinergic neurons, are rhythmic with respect to *Period* gene expression and electrical activity but do not receive direct retinal input. In contrast, some cells in the SCN core, marked by neurons containing calbindin-D28k, gastrin-releasing peptide (GRP), substance P (SP), and vasoactive intestinal polypeptide (VIP), are not rhythmic with respect to *Period* gene expression and electrical activity but do receive direct retinal input. Examination of the timing of neurogenesis using bromodeoxyuridine indicates that SCN cells are born between embryonic day 9.5 and 12.5. Calbindin, GRP, substance P, and VIP cells are born only during early SCN neurogenesis, between embryonic days 9.5–11.0. Vasopressin cells are born over the whole period of SCN neurogenesis, appearing as late as embryonic day 12.5. Examination of the ontogeny of peptide expression in these cell types reveals transient expression of calbindin in a cluster of dorsolateral SCN cells on postnatal days 1–2. The adult pattern of calbindin expression is detected in a different ventrolateral cell cluster starting on postnatal day 2. GRP and SP expression appear on postnatal day 8 and 10, respectively, after the retinohypothalamic tract has innervated the SCN. In summary, the present study describes the ontogeny-specific peptidergic phenotypes in the SCN and compares these developmental patterns to previously identified patterns in the appearance of circadian functions. These comparisons suggest the possibility that these coincident appearances may be causally related, with the direction of causation to be determined.

Keywords

Circadian rhythms; Neuropeptides; Development; Mammal; Rodent; BrdU

1. Introduction

The mammalian suprachiasmatic nucleus (SCN) controls circadian rhythmicity of many behavioral and physiological responses and synchronizes these rhythms to daily environmental cycles. It has been known for quite some time that the SCN is a heterogeneous structure composed of many different peptidergic cell types, each with a characteristic distribution within the nucleus [48]. Specific roles are now being assigned to

*Corresponding author. Department of Psychology, University of Calgary, 2500 University Drive NW, Calgary, AB, Canada T2N 1N4. Fax: +1 403 282 8249. antlem@ucalgary.ca (M.C. Antle).

these various cells [5,16,21,53]. Specifically, cells in the ventrolateral SCN that contain calbindin (CalB) and/or gastrin-releasing peptide (GRP) delineate the region in which light can induce the expression of the clock gene *Per1* [16,21]. These cells are not rhythmic in either gene expression [16] or electrical firing rate [20]. Conversely, cells in the dorsomedial region, delineated by vasopressin (VP) containing cells, rhythmically express the clock gene *Per1* but do not initially express *Per1* following a light pulse [16,53]. Recently, we have proposed a formal model whereby this organization can coordinate self-sustained rhythmicity of the SCN [4].

Determining interactions among the different SCN neurons is essential to understanding the overall function of this brain clock. One approach addressing these interactions is to compare and contrast the anatomical development of the SCN with its functional development. Mapping developmental milestones may help to reveal the functions served by individual components. Temporal coincidence between the appearance of a function and a phenotype suggests the possibility of a direct relationship. It is possible that the phenotype permits the function, or alternatively, that the function induces the phenotype. Similarly, only those phenotypes that appear either prior to or simultaneously with a function can be necessary for that function; any phenotypes appearing after a function can, at the most, only modulate that function. A number of experimental approaches have demonstrated that the SCN begins to oscillate prior to birth. In rats, the fetal SCN is rhythmic in metabolic [36–38] and in vitro electrical activity [42], although a detectable rhythm in the expression of various clock genes and their protein products is not observed until postnatal day 3 (P3; where P0 is the day of birth) [46]. A similar finding has recently been reported in hamsters [29]. Mice have rhythmic *mPer1*, but not *mPer2*, expression in the SCN prior to birth [44]. Despite the fact that rhythmic clock gene expression is not detectable in the fetal hamster [29], there is functional evidence that the hamster circadian clock is keeping time prior to birth. Fetal hamsters can be entrained in utero with injections of dopamine agonists [49] or melatonin [12,15,49], suggesting that the circadian clock is functioning prior to birth. Expression of the immediate early gene c-*fos* is activated in the SCN in utero by injections of dopamine agonists in both hamsters [49] and rats [51,52].

The appearance of light-induced c-*fos* expression in the SCN during development is species specific, with hamsters and mice first exhibiting this response on postnatal day 4 [22,24,33] while rats exhibit this response within a day of birth [25,51]. The first day during which light-induced c-*fos* expression is observed is closely associated with the arrival of retinal terminals at the SCN around P4-6 in hamsters [24,31,47] and on P1 in rats [47].

The precise timing of neurogenesis of the rodent SCN is also species specific and is related to the duration of gestation, which is shorter in hamsters (i.e., ~15.5 days) than it is in rats and mice (i.e., ~21–22 days). The cells that form the hamster SCN are born between embryonic days 9.5 and 13 (E9.5–13) [11,13] whereas cells that form the rat diencephalon are born between E13–17 [3] or later [1]. In the hamster, cells are first born in the ventral and caudal SCN, followed by those in the dorsal and rostral SCN [13]. Whether this pattern results from differences in the neurogenesis among cell phenotypes within the SCN is not known.

While nothing is currently known about the neurogenesis of different peptidergic phenotypes within the hamster SCN, there is information regarding the ontogeny of some of the peptide expression. Vasoactive intestinal polypeptide (VIP) is observed in the hamster SCN as early as E13–14 [8,40]. A similar pattern is observed in the rat, in that rostral VIP cells are present before birth, although a large population of mid-to-caudal VIP cells appear between P10 and P20 [7]. A rhythm in VIP and GRP content is detectable in rats on the day of birth [18]. VP is first found in the hamster SCN on the day of birth [40] while VP content

in rats is rhythmic at or just before birth [18,19,39]. CalB expression is observed in the SCN of mice at birth but gradually declines reaching adult expression patterns by P15 [17]. This decline in expression appears to be dependent upon retinal innervation. Such a decline has not been described in hamsters. Calretinin levels increase in the mouse SCN from birth in a pattern matching, but independent of retinal innervation of the SCN [17].

The present study examines the development of the SCN, predicting that functional heterogeneity of the SCN will be mirrored by developmental heterogeneity. By comparing the birth dates and ontogenetic appearance of cells of various peptidergic phenotypes to the appearance of a functional clock, it may be possible to better understand how individual cells that make up the SCN contribute to the generation of a coordinated rhythmic output. To this end, the present investigation was undertaken to determine the ontogeny of CalB-containing cells, as well as those bearing substance P (SP) and GRP, two proteins that are frequently colocalized with CalB [28]. Also, birthdays of cells that contain CalB, SP, GRP, VIP, and VP were determined using a bromodeoxyuridine (BrdU) protocol that labels cells as they undergo mitosis.

2. Materials and methods

2.1. Animals and housing

To study the ontogeny of SCN cells bearing different phenotypes, timed pregnant female LVG hamsters (*Mesocricetus auratus*) obtained from Charles River Breeding Labs were housed individually in translucent polypropylene cages (48 × 27 × 20 cm), exposed to a light–dark (LD) cycle of 14:10, and provided with food and water ad libitum. The room temperature was maintained at 23 ± 2 °C.

For studying neurogenesis of the different cell phenotypes, LVG hamsters were also obtained from Charles River and were similarly housed. Dark onset was defined as zeitgeber time 12 (ZT12). Starting between 7 and 10 h after dark onset (ZT19 and 22), females were paired with males and were left undisturbed for 1 h if both lordosis and intromission were observed within the first 5 min of pairing. Embryonic day 1 (E1) for the embryos was defined as precisely 4 h after dark onset (ZT16) on the night following mating. This allowed injections to occur at the same circadian phase as has been used in other studies [13].

All handling of animals was done in accordance with Institutional Animal Care and Use Committee guidelines of Columbia University.

2.2. BrdU Injections

Pregnant hamsters were injected with BrdU (Sigma, MO; 50 mg/kg in saline) once during the morning (ZT4; E9.5, 10.5, 11.5, 12.5, or 13.5) or evening (ZT16; E9.0, 10.0, 11.0, 12.0, 13.0, or 14.0), matching the phases used elsewhere [13]. BrdU readily crosses the placenta and labels any cell undergoing the S phase of mitosis within 4 h of the injection. This approach allows for the immunocytochemical identification in adults of cells born near the time of injection [41]. Pups born to these mothers were weaned at 3 weeks of age. Brains were examined immunocytochemically at 6 weeks of age.

2.3. Surgery

To enhance detection of SP, GRP, VIP, and VP in the cell soma, hamsters in the neurogenesis experiment were heavily anesthetized and given a stereotaxically aimed lateral ventricle injection of colchicine (Sigma; 200 μg in 20 μl) 1 day before being euthanized.

2.4. Perfusion

For studying the ontogeny of the various proteins, pups aged P0–P14 were given an overdose of sodium pentobarbital (0.2 mg/g) and were perfused intracardially with 5–10 ml 0.9% saline followed by 10–20 ml of Bouin's fixative in 0.1 M phosphate buffer, pH 7.3. For examining ontogeny at time points prior to birth, the pregnant dams were given an overdose of sodium pentobarbital (200 mg/kg) and perfused intracardially with 100 ml 0.9% saline followed by 300 ml of 4% paraformaldehyde. The brains were removed, postfixed for 24 h in Bouin's fixative, and cryoprotected in 30% sucrose in 0.1 M phosphate buffer for 3–5 days. Adult hamsters (6 weeks old), for both the ontogeny and neurogenesis experiments, were given an overdose of sodium pentobarbital (200 mg/kg) and were perfused intracardially with 100 ml 0.9% saline followed by 300 ml of 4% paraformaldehyde. These brains were postfixed in 4% paraformaldehyde for 24 h at 4 °C, cryoprotected in 20% sucrose in 0.1 M phosphate buffer for 3–5 days, frozen on crushed dry ice, and stored at −80 °C until used.

2.5. Immunocytochemistry

Coronal sections either 35 μm (neurogenesis experiment) or 50 μm (ontogeny experiment) were collected through the anterior hypothalamus and were processed for free floating immunocytochemistry. For the neurogenesis study, the tissue was collected into three alternating series such that three different cell phenotypes could be examined from representative sections at every rostrocaudal level of the SCN.

For the ontogeny experiment, brains were rinsed in 0.5% H_2O_2, incubated for 1 h in 1% normal serum, and then incubated for 48 h in either monoclonal mouse-anti-CalB (1:20,000, Sigma), polyclonal rabbit-anti-GRP (1:2,000, Incstar, MN), or polyclonal rabbit-anti-SP (1:10,000, Incstar). Tissue was then incubated in a secondary antibody, followed by ABC (Vector Labs, CA), and was stained with either the Vector SG substrate kit for peroxidase, or with DAB. Sections were mounted onto gelatin coated slides, dehydrated with an alcohol series, cleared with Citrasolve, and coverslipped with Permount.

For the neurogenesis study, sections were subjected to the following treatments: Tris-buffered saline (TBS, pH 7.4) washes, 2 h wash in 50% formamide/2× saline-sodium citrate (SSC) at 65 °C, rinsed in 2× SSC, soaked in 2 N HCl for 30 min at 37 °C, soaked in 0.1 M borate buffer (pH 8.5), and blocked in 3% normal donkey serum in TBS with 0.1% Triton X-100 (TBS-plus). The tissue was incubated for 48 h at 4 °C in TBS-plus containing monoclonal mouse-anti-BrdU IgG (1:1000 Sigma), and one or two of the following antibodies: rabbit anti-CalB (1:3300, Chemicon), rabbit-anti-VIP (1:5000, Peninsula Labs), rabbit-anti-VP (1:5000, DiaSorin), or guinea pig anti-SP (1:2500, Peninsula Labs). Following incubation, the tissue was rinsed in phosphate-buffered saline (PBS, pH7.4) containing 0.1% Triton X-100 (0.1% PBT), and incubated in fluorescent secondary antibodies (1:200, CY3 conjugated donkey-anti-mouse; CY2 or CY5 conjugated donkey-anti-rabbit; and CY2 donkey-anti-guinea pig; Jackson Immunochemicals Inc., PA). The tissue was rinsed in 0.1% PBT, mounted onto gelatin coated slides, dehydrated through an alcohol series, cleared with xylene, and coverslipped with Krystalon.

2.6. Data analysis

SG or DAB-labeled tissue was examined on an Olympus BH-2 microscope. Fluorescently labeled tissue was examined on an epifluorescent-equipped Nikon Eclipse 800 microscope. In each case, images were captured on a cooled CCD camera mounted on the microscope. Each fluorescent label was imaged separately, and the channels were merged to form red-green pseudo-color images.

High magnification images of representative double-labeled cells were captured using confocal microscopy. The slides were observed under a Zeiss Axiovert 200 MOT fluorescence microscope (Carl Zeiss, Thornwood, NY, USA) with a Zeiss LSM 510META laser scanning confocal attachment. The sections were excited with an argon–krypton laser using the excitation wavelengths 488 nm for Cy2, 543 nm for Cy3, and 633 nm for Cy5. The images were collected as 2 μm multitract optical sections with sequential excitation by each laser to avoid crosstalk between the three wavelengths. Using the LSM Image Browser 3.2 software (Zeiss), the images captured from the Cy3 signal were given a red pseudo-color, while images captured from the Cy2 or Cy5 signals were given green pseudo-color. Each cell was examined through its entirety to verify that it was double labeled.

Cell counts were made of 4–6 sections covering the rostrocaudal extent of the SCN. Individual cells in each photomicrograph were identified by examining digitally captured images with Adobe Photoshop by removing the color channel corresponding to the BrdU label. Once each cell was marked, the channel corresponding to the phenotype label was removed, and the channel with the BrdU was compared to the markers representing individual cell. When a BrdU-labeled nucleus coincided with a cell marker, the individual cell was also examined with both channels active to ensure that the BrdU-labeled nucleus actually corresponded to that particular cell. Total counts were made through the whole rostrocaudal extent of the SCN for each of the 5 phenotypic markers. Total counts of double-labeled cells in a particular animal for a specific cell phenotype were expressed as a percentage of total number of cells for the given phenotype in the given animal. One-way ANOVAs were applied to each phenotype to test for a main effect of day of BrdU injection, and Fisher's LSD post hoc tests were used to examine pairwise differences when a main effect was detected.

Cell size measurements were made of rostral VP cells (near the 3rd ventricle in the rostral half of the nucleus), caudal VP cells (along midline at the rostrocaudal level of the CalB subregion), and CalB cells labeled with DAB in tissue from two colchicine-treated animals. Measurements (area, perimeter, and diameter) were made using the NIH-Image software package. Ten to 12 cells were measured per animal. *T* tests were used to compare these measurements.

3. Results

3.1. Ontogeny phenotypic proteins

On E14 and 15, densely stained CalB-immunoreactive (-ir) cells surrounded the SCN and were present in the subparaventricular zone, but not in the SCN. A few CalB-ir fibers were seen in the SCN. These fibers seem to project from the cells surrounding the SCN, as a few can be traced to those cell bodies. CalB-ir cells first appeared in the SCN on P1. A distinct cluster of cells was detected in the dorsolateral region of the caudal SCN (Fig. 1). Sparse cells were also present in the rostral, dorsomedial, and ventrolateral SCN. On P2, in addition to the dorsomedial cells, CalB-containing cells were apparent in the ventrolateral region of the caudal SCN. While extra-SCN CalB-ir cells were intensely stained, those within the SCN were less intensely labeled at this age. At P3, CalB-ir had disappeared from most of the cells in the dorsolateral cluster while the ventrolateral cluster of CalB cells had become more distinct. Over the following days, CalB was increasingly localized to cells in the ventrolateral region, reaching the adult pattern by P15.

A few GRP-ir cells were observed in 1 of the 4 animals examined at P8 (Fig 2). A small group of GRP-ir cells was distinct in the ventrolateral region of the caudal SCN in all animals at P10. Denser background staining was seen in all 4 animals at P10 and P12 in the latero-caudal SCN. At P14, GRP fibers were detected in this same region of the SCN (data

not shown), suggesting that the background staining observed on P10 and P12 represented initial GRP-ir fibers. This pattern of heavy GRP-ir in the dorsolateral SCN is typical of what is expected in SCN tissue from animals that have not received colchicine treatment [28]. SP-ir fibers were seen surrounding the SCN at P3 (the earliest time processed for SP ICC) and a few fibers were seen entering the SCN. SP-ir cells were first detected at P10. By P12 a distinct cell cluster was found in the ventrolateral caudal SCN (Fig 3). It is possible that these peptides appear earlier, but at levels that are undetectable using the present immunocytochemistry protocols.

3.2. Neurogenesis of different cell phenotypes

BrdU-labeled cells were observed first in the ventral portion of the mid-caudal SCN. On the final days during which BrdU was found in the SCN, labeled cells were located in the dorsomedial SCN along the whole rostrocaudal extent, although in greater numbers in the rostral SCN (Fig. 4).

The patterns of neurogenesis for CalB, GRP, and SP were quite similar. The first BrdU-labeled CalB cells were observed in animals injected on E9.5 (Fig 5), with a significant increase ($F(7,28) = 23.6$, $P < 0.001$) to the largest number of double-labeled cells observed on E10.5–11.0 (Fig. 6A), after which there was a significant drop to almost no double-labeled cells from E11.5 onwards. The first few BrdU-labeled GRP cells were observed in animals injected on E9.0, with a significant increase ($F(5,9) = 31.2$, $P < 0.001$) to the largest number of double-labeled cells observed on E10.5–11.0 (Fig. 6A), after which there was a significant drop to almost no double-labeled cells from E11.5 onwards. The first BrdU-labeled SP cells were observed in animals injected on E9.5. The number of BrdU-labeled SP cells increased slightly to a peak on E11.0 (Fig. 6A) after which there was a significant drop to ($F(5,8) = 7.2$, $P < 0.01$) almost no double-labeled cells from E11.5 onwards.

The first few BrdU-labeled VIP cells were observed in animals injected on E9.0. The number of BrdU-labeled VIP cells increased to a significant peak ($F(6,12) = 12.8$, $P < 0.001$) on E10.5 (Fig. 6A), after which there was a gradual drop to almost no double-labeled cells from E12.0 onwards.

The most dramatic finding regarding neurogenesis was observed with VP cells. Unlike all other cell phenotypes examined, BrdU-labeled VP cells were observed over the whole range of SCN neurogenesis from E9.0 through to E12.5. The overall shape of the neurogenesis curve was more broad and flat than that for the other cell phenotypes. The peak in the neurogenesis curve was not as prominent as was observed with the other cell phenotypes, although there was a significant increasing trend ($F(6,11) = 7.2$, $P < 0.01$) from E9.0 to a broad peak covering E10.5 to E11.5 (Fig. 6A), after which there was a gradual decline in number to E13.0, at which point no BrdU-labeled cells were observed in the SCN. While the neurogenesis curve may suggest a homogeneous and prolonged pattern or cell birth, regional examination of BrdU-labeled cell location indicates that the caudal VP cells predominate early in neurogenesis, while the rostral VP predominate later in neurogenesis. The cell size of rostral and caudal VP cells did not differ for any measurement (area, 50.18 μm^2 vs. 47.15 μm^2, $P > 0.05$; perimeter, 27.44 μm vs. 26.39 μm, $P > 0.05$; diameter, 9.67 μm vs. 9.09 μm, $P > 0.05$). By comparison, CalB cells were significantly larger than both rostral and caudal VP cells on most measurement (area, 60.28; perimeter, 30.87; diameter, 11.37). Only the area of rostral VP cells was not significantly smaller than that of CalB cells (one-tailed *t* test, $P = 0.069$).

4. Discussion

The present study demonstrates that CalB-, GRP-, SP-, and VIP-containing cells are born in the first wave of SCN neurogenesis, while VP-containing cells appear over the entire period of neurogenesis. These VP-ergic cells are born in a specific spatiotemporal manner; caudal VP-containing cells predominate early in neurogenesis, while rostral VP-containing cells, particularly those close to the third ventricle, predominate later in neurogenesis. This matches well the overall general pattern of neurogenesis described previously [11,13]. These developmental differences observed in VP cells are not echoed by any known differences between these cell populations. While the present study identified VP-containing cells as being the last born during SCN neurogenesis, a recent report in the rat detected CalB and VIP cells that were born on E18 [1], well after the end of the previously identified neurogenesis period in rats (i.e., E13–17 [3]). In the present study, animals were injected with BrdU as late as E13.5 and E14.0 (~36–48 h before birth). These animals had no BrdU-labeled cells in their SCN (data not shown), suggesting that hamsters do not exhibit additional late neurogenesis such as has been reported in the rat [1].

Surprisingly, the detection of neurons with various peptidergic phenotypes occurs over a wide interval; from E13 for VIP [8], through P0–1 for VP [40] and CalB, to P8–10 for the first appearance of GRP and SP. It is known that CalB is often colocalized with GRP or SP [28], yet these colocalized peptides are detected at different times during ontogeny. It has been suggested that in the adult, CalB cells act as gates that maintain phase coherence among SCN oscillator cells [4]. It is possible that synchrony among oscillator cells is maintained in utero by a maternal signal. Pups are normally synchronized to one another at birth. This is not the case for pups born to SCN lesioned mothers, suggesting that there is a maternal signal that entrains the pups [38]. Given that synaptogenesis largely occurs after birth [30], it is reasonable to suggest that SCN neurons may be unable to maintain synchrony amongst themselves, and that the entraining maternal zeitgeber may also control the phase of the individual SCN oscillator cells, not just the phase of the fetuses. If the hypothesis that CalB cells maintain such synchrony in adults is correct, then possibly CalB cells appearing soon after birth are related to initiation of this synchronization function. The appearance of GRP and SP soon after the retinohypothalamic tract (RHT) innervates the SCN suggests that these peptides may play a role in photic regulation of rhythmicity, or that retinal innervation may play a role in their appearance. The developmental patterns of these various SCN attributes are summarized in Fig. 6B.

An interesting observation made in the present studies was that a dorsolateral cluster of neurons within the SCN contain CalB only between P1 and P2. Transient expression of CalB has been described in the mouse SCN, where the number of CalB-ir neurons decreases as the RHT innervates the SCN [17]. This transient dorsolateral cluster of CalB-ir cells is located in the region expressing phosphorylated extracellular signal-regulated kinase (P-ERK) at night in the adult hamster [10,26,34]. Phosphorylation of ERK has been implicated in photic resetting [9,10,14]. The role served by the transient expression of CalB early in development in these dorsolateral SCN cells is unknown. Furthermore, it is not known whether the disappearance of CalB is due to change in expression patterns within these cells, or due to cell death.

Soon after neurogenesis, yet before synaptogenesis, the SCN is endogenously rhythmic [36–38] and can be synchronized with timed injections of dopamine agonists or melatonin [49,50]. At this early age, VIP-ergic cells are already found in the SCN [8], but no CalB-ir can be detected. In the rat, the earliest expressions of overt rhythms have been demonstrated in body temperature and oxygen consumption at P5 [32]. As VIP, VP, CalB, and glial cells are present prior to P5, these cell types may contribute to the expression of overt

rhythmicity. Indeed, lesions of the region containing CalB cells in adult hamsters are sufficient to abolish overt rhythms in behavioral and physiological responses [23,27]. Transplants of partial SCN grafts containing CalB cells restore activity rhythms in SCN lesioned hamsters, while SCN grafts lacking these cells do not lead to such a recovery [27]. This arrangement has been incorporated into a model where CalB cells are triggered to produce a daily signal that maintains phase coherence amongst individual oscillating cells of the SCN [4]. It is possible that endogenous signals from the mother initially produce and maintain phase coherence of individual rhythmic cells [38]. According to this hypothesis, following birth, but prior to RHT innervation, the CalB cells would maintain phase coherence as outlined in the model [4]. Finally, once the RHT innervates the SCN, daily photic signals would strengthen and maintain this phase coherence.

GRP and SP-containing cells are detected around at P8-10, after the RHT has begun to innervate the SCN. Although it is not known if RHT innervation induces the expression of the proteins, it has been shown that these peptides serve a role in light-induced responses. Indeed, administration of GRP phase shifts locomotor activity with a phase–response curve similar to light [35]. GRP injections induce *Per1* gene expression in the SCN [2,6] and GRP receptor-deficient mice show blunted *Per1* expression and phase shifts [2]. SP produces phase shifts in SCN electrical firing rhythms in vitro with a phase response curve similar to light [43]. This region containing CalB, GRP, and SP cells expresses light-induced, but not rhythmic, *Per1* and *Per2* expression in adult hamsters [16]. This is also the region expressing most light-induced c-*fos* in adult hamsters [45]. Curiously, light-induced c-*fos* first appears predominantly in the dorsolateral hamster SCN on P4, and only later, around P15, is light-induced c-*fos* predominantly in the ventrolateral SCN [22]. Therefore, the developmental pattern of light-induced c-*fos* expression in the hamster SCN follows, with some delay, the developmental pattern of CalB-ir.

In conclusion, the ontogeny of GRP- and SP-containing SCN cells and the pharmacological effects of these peptides in adults are consistent with a role in photic entrainment and phase shifting. CalB is frequently colocalized with GRP or SP in the adult SCN. In development, however, CalB is detected at an earlier developmental stage than are the latter peptides. The appearance of CalB soon after birth may be related to the loss of maternal zeitgebers. It has been suggested that CalB cells of the SCN maintain phase coherence among individual oscillator cells in the adult hamster [4,23]. While maternal zeitgebers may serve this function prior to birth [38], it is possible that the CalB cells that appear soon after birth maintain phase coherence in the postnatal period. Further investigation will be required to assess this hypothesis.

Acknowledgments

This work was supported by NIH grant #37919 (RS) and by fellowships from NSERC and CIHR (MCA). We thank Carrie Wright and Mohammad Ali for excellent technical assistance and Melissa M. Holmes for assistance with the BrdU protocol.

References

1. Abizaid A, Mezei G, Sotonyi P, Horvath TL. Sex differences in adult suprachiasmatic nucleus neurons emerging late prenatally in rats. Eur J Neurosci. 2004; 19:2488–2496. [PubMed: 15128402]
2. Aida R, Moriya T, Araki M, Akiyama M, Wada K, Wada E, Shibata S. Gastrin-releasing peptide mediates photic entrainable signals to dorsal subsets of suprachiasmatic nucleus via induction of *Period* gene in mice. Mol Pharmacol. 2002; 61:26–34. [PubMed: 11752203]
3. Altman J, Bayer SA. Development of the diencephalon in the rat: I. Autoradiographic study of the time of origin and settling patterns of neurons of the hypothalamus. J Comp Neurol. 1978; 182:945–971. [PubMed: 103939]

4. Antle MC, Foley DK, Foley NC, Silver R. Gates and oscillators: a network model of the brain clock. J Biol Rhythms. 2003; 18:339–350. [PubMed: 12932086]
5. Antle MC, Silver R. Orchestrating time: Arrangements of the brain circadian clock. Trends Neurosci. 2005; 28:145–151. [PubMed: 15749168]
6. Antle MC, Kriegsfeld LJ, Silver R. Signaling within the brain's master clock: Localized activation of MAP kinase by gastrin-releasing peptide. J Neurosci. 2005; 25:2447–2454. [PubMed: 15758152]
7. Ban Y, Shigeyoshi Y, Okamura H. Development of vasoactive intestinal peptide mRNA rhythm in the rat suprachiasmatic nucleus. J Neurosci. 1997; 17:3920–3931. [PubMed: 9133410]
8. Botchkina GI, Morin LP. Ontogeny of radial glia, astrocytes and vasoactive intestinal peptide immunoreactive neurons in hamster suprachiasmatic nucleus. Brain Res, Dev Brain Res. 1995; 86:48–56.
9. Butcher GQ, Dziema H, Collamore M, Burgoon PW, Obrietan K. The p42/44 mitogen-activated protein kinase pathway couples photic input to circadian clock entrainment. J Biol Chem. 2002; 277:29519–29525. [PubMed: 12042309]
10. Coogan AN, Piggins HD. Circadian and photic regulation of phosphorylation of ERK1/2 and Elk-1 in the suprachiasmatic nuclei of the Syrian hamster. J Neurosci. 2003; 23:3085–3093. [PubMed: 12684495]
11. Crossland WJ, Uchwat CJ. Neurogenesis in the central visual pathways of the golden hamster. Brain Res. 1982; 281:99–103. [PubMed: 7139343]
12. Davis FC, Mannion J. Entrainment of hamster pup circadian rhythms by prenatal melatonin injections to the mother. Am J Physiol. 1988; 255:R439–R448. [PubMed: 3414839]
13. Davis FC, Boada R, LeDeaux J. Neurogenesis of the hamster suprachiasmatic nucleus. Brain Res. 1990; 519:192–199. [PubMed: 2397405]
14. Dziema H, Oatis B, Butcher GQ, Yates R, Hoyt KR, Obrietan K. The ERK/MAP kinase pathway couples light to immediate-early gene expression in the suprachiasmatic nucleus. Eur J Neurosci. 2003; 17:1617–1627. [PubMed: 12752379]
15. Grosse J, Velickovic A, Davis FC. Entrainment of Syrian hamster circadian activity rhythms by neonatal melatonin injections. Am J Physiol. 1996; 270:R533–R540. [PubMed: 8780217]
16. Hamada T, LeSauter J, Venuti JM, Silver R. Expression of Period genes: rhythmic and nonrhythmic compartments of the suprachiasmatic nucleus pacemaker. J Neurosci. 2001; 21:7742–7750. [PubMed: 11567064]
17. Ikeda M, Allen CN. Developmental changes in calbindin-D28k and calretinin expression in the mouse suprachiasmatic nucleus. Eur J Neurosci. 2003; 17:1111–1118. [PubMed: 12653988]
18. Isobe Y, Muramatsu K. Day–night differences in the contents of vasoactive intestinal peptide, gastrin-releasing peptide and Arg-vasopressin in the suprachiasmatic nucleus of rat pups during postnatal development. Neurosci Lett. 1995; 188:45–48. [PubMed: 7783976]
19. Isobe Y, Nakajima K, Nishino H. Arg-vasopressin content in the suprachiasmatic nucleus of rat pups: circadian rhythm and its development, Brain Res. Dev Brain Res. 1995; 85:58–63. [PubMed: 7781168]
20. Jobst EE, Allen CN. Calbindin neurons in the hamster suprachiasmatic nucleus do not exhibit a circadian variation in spontaneous firing rate. Eur J Neurosci. 2002; 16:2469–2474. [PubMed: 12492442]
21. Karatsoreos IN, Yan L, LeSauter J, Silver R. Phenotype matters: identification of light-responsive cells in the mouse suprachiasmatic nucleus. J Neurosci. 2004; 24:68–75. [PubMed: 14715939]
22. Kaufman CM, Menaker M. Ontogeny of light-induced Fos-like immunoreactivity in the hamster suprachiasmatic nucleus. Brain Res. 1994; 633:162–166. [PubMed: 8137152]
23. Kriegsfeld LJ, LeSauter J, Silver R. Targeted microlesions reveal novel organization of the hamster suprachiasmatic nucleus. J Neurosci. 2004; 24:2449–2457. [PubMed: 15014120]
24. Lavialle M, Serviere J. Developmental study in the circadian clock of the golden hamster: a putative role of astrocytes, Brain Res. Dev Brain Res. 1995; 86:275–282. [PubMed: 7656420]
25. Leard LE, Macdonald ES, Heller HC, Kilduff TS. Ontogeny of photic-induced c-*fos* mRNA expression in rat suprachiasmatic nuclei. NeuroReport. 1994; 5:2683–2687. [PubMed: 7696632]

26. Lee HS, Nelms JL, Nguyen M, Silver R, Lehman MN. The eye is necessary for a circadian rhythm in the suprachiasmatic nucleus. Nat Neurosci. 2003; 6:111–112. [PubMed: 12536213]
27. LeSauter J, Silver R. Localization of a suprachiasmatic nucleus subregion regulating locomotor rhythmicity. J Neurosci. 1999; 19:5574–5585. [PubMed: 10377364]
28. LeSauter J, Kriegsfeld LJ, Hon J, Silver R. Calbindin-D(28K) cells selectively contact intra-SCN neurons. Neuroscience. 2002; 111:575–585. [PubMed: 12031345]
29. Li, X.; Davis, FC. Society for research on biogical rhythms (Abstracts). Whistler, BC: 2004. Expression of clock genes in the hamster SCN during development; p. 105
30. Moore RY, Bernstein ME. Synaptogenesis in the rat suprachiasmatic nucleus demonstrated by electron microscopy and synapsin I immunoreactivity. J Neurosci. 1989; 9:2151–2162. [PubMed: 2498469]
31. Muller C, Torrealba F. Postnatal development of neuron number and connections in the suprachiasmatic nucleus of the hamster, Brain Res. Dev Brain Res. 1998; 110:203–213. [PubMed: 9748579]
32. Mumm B, Kaul R, Heldmaier G, Schmidt I. Endogenous 24-h cycle of core temperature and oxygen consumption in week-old Zucker rat pups. J Comp Physiol, B. 1989; 159:569–575. [PubMed: 2607019]
33. Munoz Llamosas M, Huerta JJ, Cernuda-Cernuda R, Garcia-Fernandez JM. Ontogeny of a photic response in the retina and suprachiasmatic nucleus in the mouse. Brain Res, Dev Brain Res. 2000; 120:1–6.
34. Obrietan K, Impey S, Storm DR. Light and circadian rhythmicity regulate MAP kinase activation in the suprachiasmatic nuclei. Nat Neurosci. 1998; 1:693–700. [PubMed: 10196585]
35. Piggins HD, Antle MC, Rusak B. Neuropeptides phase shift the mammalian circadian pacemaker. J Neurosci. 1995; 15:5612–5622. [PubMed: 7643205]
36. Reppert SM, Schwartz WJ. Maternal coordination of the fetal biological clock in utero. Science. 1983; 220:969–971. [PubMed: 6844923]
37. Reppert SM, Schwartz WJ. The suprachiasmatic nuclei of the fetal rat: characterization of a functional circadian clock using 14C-labeled deoxyglucose. J Neurosci. 1984; 4:1677–1682. [PubMed: 6737036]
38. Reppert SM, Schwartz WJ. Maternal suprachiasmatic nuclei are necessary for maternal coordination of the developing circadian system. J Neurosci. 1986; 6:2724–2729. [PubMed: 3746430]
39. Reppert SM, Uhl GR. Vasopressin messenger ribonucleic acid in supraoptic and suprachiasmatic nuclei: appearance and circadian regulation during development. Endocrinology. 1987; 120:2483–2487. [PubMed: 3569140]
40. Romero MT, Silver R. Time course of peptidergic expression in fetal suprachiasmatic nucleus transplanted into adult hamster. Brain Res, Dev Brain Res. 1990; 57:1–6.
41. Sadikot AF, Sasseville R. Neurogenesis in the mammalian neo-striatum and nucleus accumbens: parvalbumin-immunoreactive GABAergic interneurons. J Comp Neurol. 1997; 389:193–211. [PubMed: 9416916]
42. Shibata S, Moore RY. Development of neuronal activity in the rat suprachiasmatic nucleus. Brain Res. 1987; 431:311–315. [PubMed: 3040191]
43. Shibata S, Tsuneyoshi A, Hamada T, Tominaga K, Watanabe S. Effect of substance P on circadian rhythms of firing activity and the 2-deoxyglucose uptake in the rat suprachiasmatic nucleus in vitro. Brain Res. 1992; 597:257–263. [PubMed: 1282077]
44. Shimomura H, Moriya T, Sudo M, Wakamatsu H, Akiyama M, Miyake Y, Shibata S. Differential daily expression of *Per1* and *Per2* mRNA in the suprachiasmatic nucleus of fetal and early postnatal mice. Eur J Neurosci. 2001; 13:687–693. [PubMed: 11207804]
45. Silver R, Romero MT, Besmer HR, Leak R, Nunez JM, LeSauter J. Calbindin-D28K cells in the hamster SCN express light-induced Fos. NeuroReport. 1996; 7:1224–1228. [PubMed: 8817537]
46. Sladek M, Sumova A, Kovacikova Z, Bendova Z, Laurinova K, Illnerova H. Insight into molecular core clock mechanism of embryonic and early postnatal rat suprachiasmatic nucleus. Proc Natl Acad Sci U S A. 2004; 101:6231–6236. [PubMed: 15069203]

47. Speh JC, Moore RY. Retinohypothalamic tract development in the hamster and rat. Brain Res, Dev Brain Res. 1993; 76:171–181.

48. van den Pol AN, Tsujimoto KL. Neurotransmitters of the hypothalamic suprachiasmatic nucleus: immunocytochemical analysis of 25 neuronal antigens. Neuroscience. 1985; 15:1049–1086. [PubMed: 2413388]

49. Viswanathan N, Davis FC. Single prenatal injections of melatonin or the D1-dopamine receptor agonist SKF 38393 to pregnant hamsters sets the offsprings' circadian rhythms to phases 180 degrees apart. J Comp Physiol, A. 1997; 180:339–346. [PubMed: 9106997]

50. Viswanathan N, Weaver DR, Reppert SM, Davis FC. Entrainment of the fetal hamster circadian pacemaker by prenatal injections of the dopamine agonist SKF 38393. J Neurosci. 1994; 14:5393–5398. [PubMed: 7916044]

51. Weaver DR, Reppert SM. Definition of the developmental transition from dopaminergic to photic regulation of c-*fos* gene expression in the rat suprachiasmatic nucleus. Brain Res, Mol Brain Res. 1995; 33:136–148. [PubMed: 8774955]

52. Weaver DR, Rivkees SA, Reppert SM. D1-dopamine receptors activate c-*fos* expression in the fetal suprachiasmatic nuclei. Proc Natl Acad Sci U S A. 1992; 89:9201–9204. [PubMed: 1384044]

53. Yan L, Silver R. Differential induction and localization of *mPer1* and *mPer2* during advancing and delaying phase shifts. Eur J Neurosci. 2002; 16:1531–1540. [PubMed: 12405967]

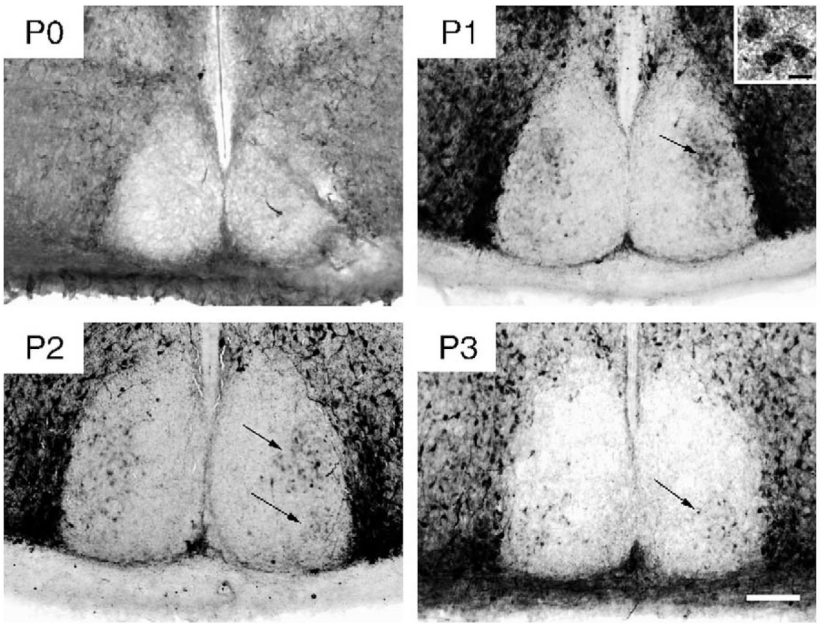

Fig. 1.

Photomicrographs of CalB-ir in the caudal SCN on P0, P1, P2, and P3. The black arrows indicate both the dorsolateral and ventrolateral cluster of CalB cells (visible on P1–2 and P2–3, respectively) (Scale bar = 100 μm). Inset in P1 photomicrograph shows 3 CalB-IR cells at high power (Scale bar = 10 μm).

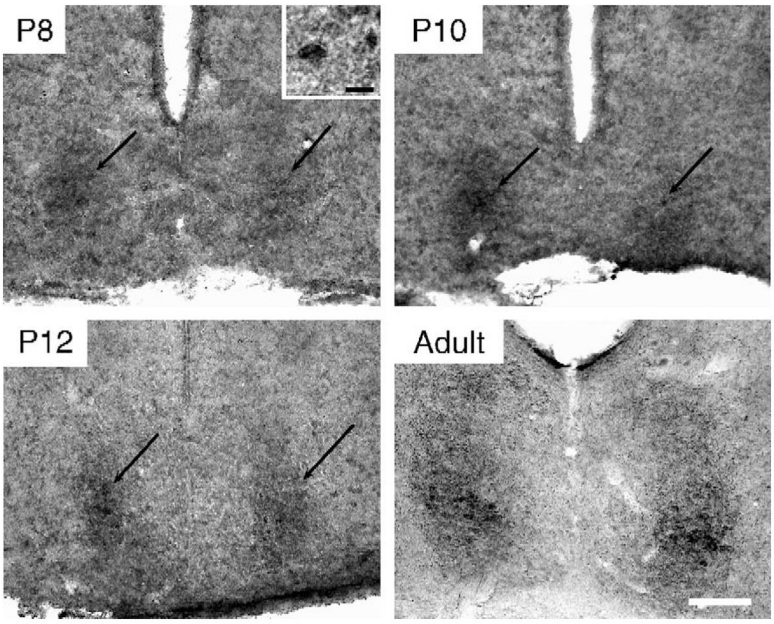

Fig. 2.

Photomicrographs of GRP-ir in the caudal SCN on P8, P10, and P12 and in a young adult. The black arrows indicate the location of the GRP-ir cluster of SCN cells, first visible on P8 (Scale bar = 100 μm). Inset in P8 photomicrograph shows a GRP-ir cell at high power (Scale bar = 10 μm).

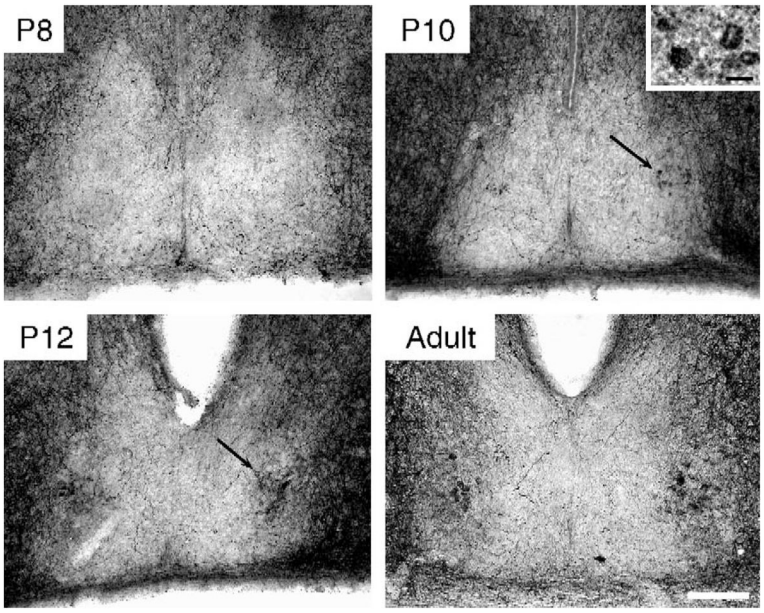

Fig. 3.

Photomicrographs of SP-ir in the caudal SCN on P8, P10, and P12 and in a young adult. The black arrows indicate the location of SP-ir cells, first visible on P10 (Scale bar = 100 μm). Inset in P10 photomicrograph shows 4 SP-ir cells at high power (Scale bar = 10 μm).

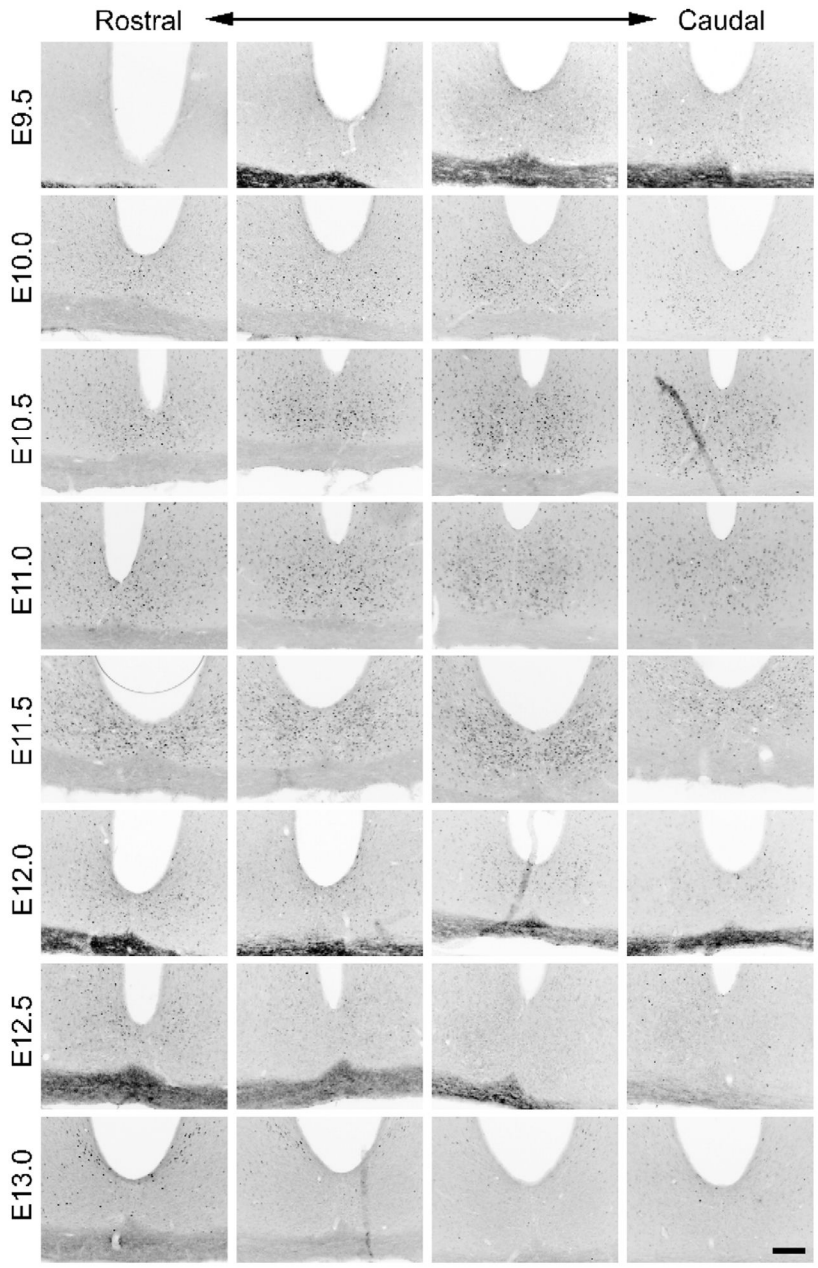

Fig. 4.

Photomicrographs depicting BrdU-ir at 4 different rostrocaudal levels of the SCN at half-day intervals throughout the neurogenesis period for the SCN. Ventral BrdU-ir most prevalent in the early stages of neurogenesis (E10.0–10.5), while dorsal BrdU-ir is more prevalent in the later stages of neurogenesis (E11.5–12.0). Caudal BrdU-ir is more prevalent in the early stages of neurogenesis (E10.5), while rostral BrdU-ir is more prevalent in the later stages of neurogenesis (E11.5) (Scale bar = 100 μm).

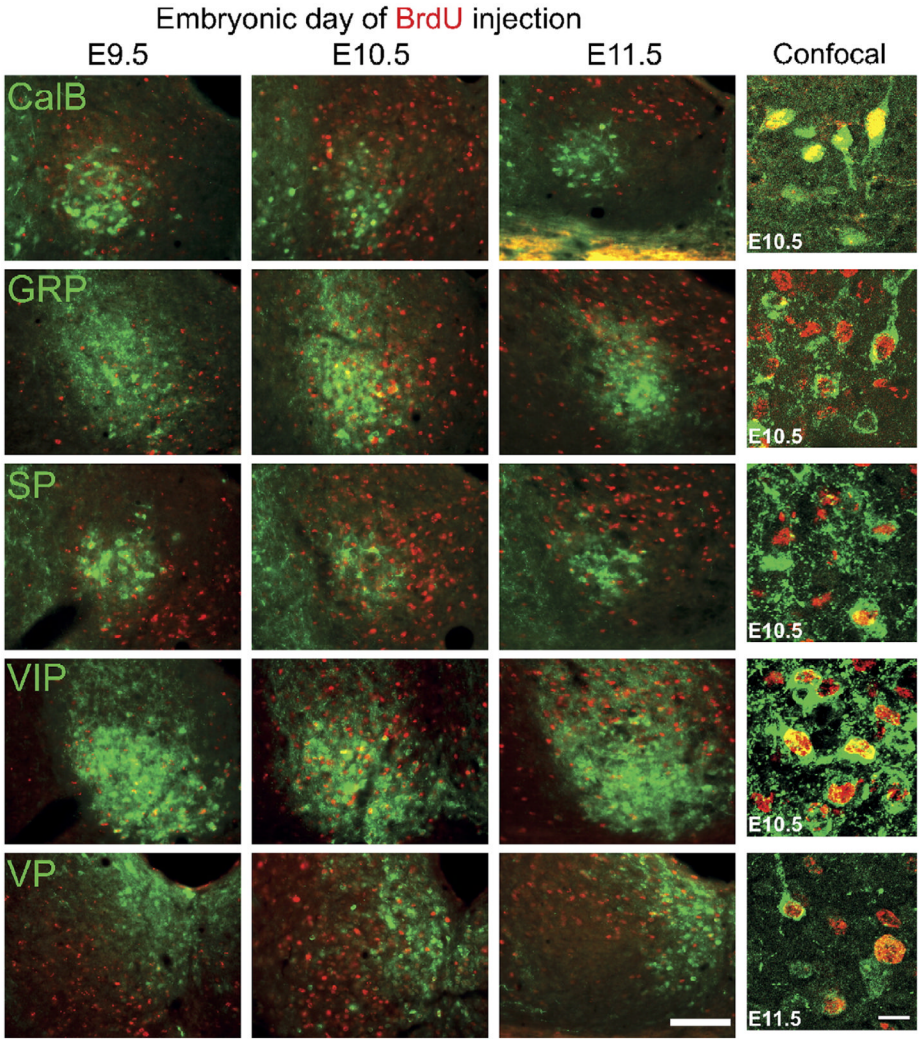

Fig. 5.

Double-labeled immunofluorescent photomicrographs depicting the pattern of neurogenesis (BrdU-ir cells in red) relative to the spatial distribution of the various cell phenotype (CalB, GRP, SP, VIP, and VP, in green). Each column represents data from animals injected with BrdU at one of three stages of SCN neurogenesis: early (E9.5), peak (E10.5), and late (E11.5). Note that BrdU-ir is sparse and ventral on E9.5, more dense on E10.5, and is sparse and dorsal on E11.5 (Scale bar = 100 μm). The right column shows 2 μm thick optical section obtained using confocal microscopy depicting BrdU and peptidergic-ir colocalization (Scale bar = 10 μm). (For interpretation of the references to colour in this figure legend, the reader is referred to the web version of this article.)

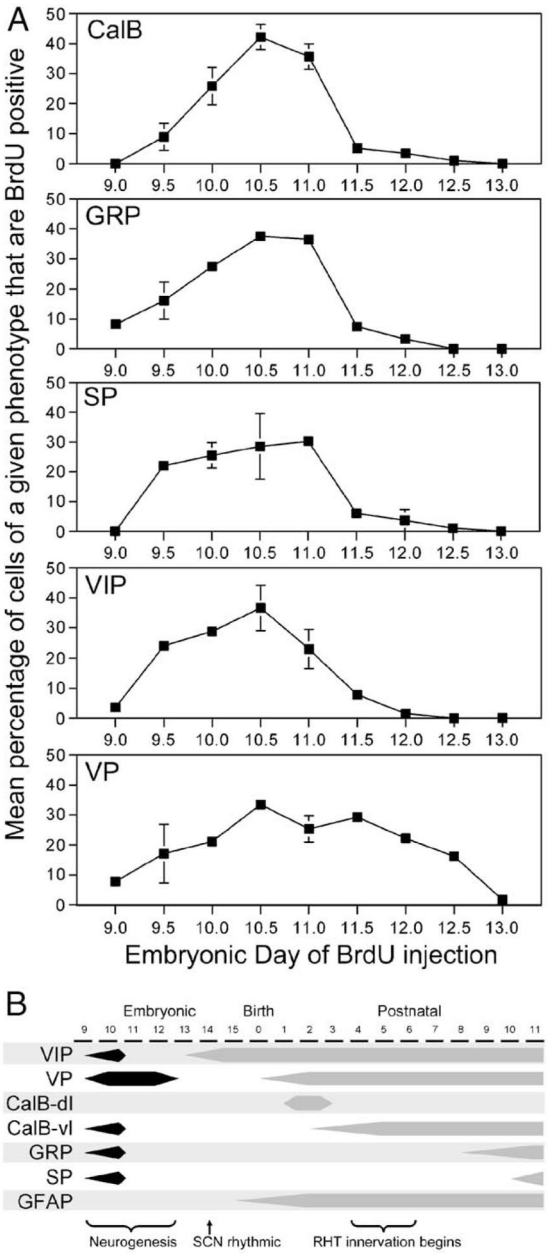

Fig. 6.

(A) Plots depicting the neurogenetic pattern of cells that, in adulthood, contain CalB, GRP, SP, VIP, and VP. The embryonic day of the BrdU injection is indicated along the abscissa. The ordinate indicates the average percentage of cells immunoreactive for the peptide of interest that are also immunoreactive for BrdU. (B) A schematic outlining important developmental milestones of SCN attributes, including those described here (neurogenesis, and the ontogeny of detectable expression of CalB, GRP and SP) as well as elsewhere (neurogenesis [11,13]; VIP-ir [8]; SCN rhythmicity [12,36,49]; GFAP-ir [8]; VP-ir [40]; and RHT innervation [24,31,47]).